Tissue spheroid fusion-based in vitro screening assays for analysis of tissue maturation

Zoltan Hajdu[*], **Vladimir Mironov**[*], **Agnes Nagy Mehesz**, **Russell A. Norris**, **Roger R. Markwald**, and **Richard P. Visconti**[¶]

Department of Cell Biology and Anatomy, Medical University of South Carolina, Charleston, South Carolina, USA

Abstract

Organ printing or computer-aided robotic layer by layer additive biofabrication of thick three-dimensional living tissue constructs employing self-assembling tissue spheroids is a rapidly evolving alternative to classic solid scaffold-based approaches in tissue engineering. However, the absence of effective methods of accelerated tissue maturation immediately after bioprinting is the main technological imperative and potential impediment for further progress in the development of this emerging organ printing technology. Identification of the optimal combination of factors and conditions that accelerate tissue maturation ("maturogenic" factors) is an essential and necessary endeavor. Screening of maturogenic factors would be most efficiently accomplished using high throughput quantitative in vitro tissue maturation assays. We have recently reviewed the formation of solid scaffold-free tissue constructs through fusion of bioprinted tissue spheroids that have measurable material properties. We hypothesize that the fusion kinetics of these tissue spheroids will provide an efficacious in vitro assay of the level of tissue maturation. Herein, we report the results of experimental testing of two simple quantitative tissue spheroid fusion-based in vitro high throughput screening assays of tissue maturation: i) a tissue spheroid envelopment assay; and ii) a tissue spheroid fusion kinetics assay.

Keywords

tissue spheroid; fibroblast; maturogen; biofabrication; fusion kinetics; tissue engineering

Organ printing is defined as computer-aided robotic additive biofabrication of thick 3D living tissue constructs using self-assembling tissue spheroids as building blocks (Mironov et al. 2003; Mironov et al. 2008; Mironov et al. 2009). Sequential (layer-by-layer) spraying or deposition of hydrogel layers ("biopaper") combined with robotic punching or dispensing (precise placement) of tissue spheroids ("bioink") with a diameter corresponding to the thickness of the sprayed hydrogel layer guided by computer-aided design ("blueprint") constitutes the essence of 3D organ printing technology that, in certain aspects, resembles traditional 2D printing invented by Johannes Gutenberg in Europe several centuries ago (Mironov et al. 2008). Tissue fusion of fluid-like tissue spheroids or tissue self-assembly, driven by surface tension forces, is the fundamental biological and biophysical principle of organ printing technology (Jakab et al. 2004; Marga et al. 2007; Jakab et al. 2008; Jakab et al. 2008; Mironov et al. 2008; Mironov et al. 2009). Organ printing, a solid scaffold-free

---

[¶]Corresponding author: Department of Cell Biology and Anatomy, Medical University of South Carolina, 173 Ashley Avenue – CRI605a, Mail Stop 250508, Charleston, South Carolina, 29425 USA. visconrp@musc.edu Phone: 843-792-6024; FAX: 843-792-0664.
[*] = equal contribution

Conflict of Interest: None

method of tissue construction, could potentially prove to be a superior technological alternative to classic solid scaffold-based approaches in tissue engineering [Mironov et al. 2008, Mironov et al. 2009]. However, solid scaffold-free tissue-engineering approaches can only be effectively implemented if optimal methods of accelerated tissue maturation can be developed. Rapid tissue maturation or transition of bioprinted 3D tissue constructs from the fluid-like state of tissue spheroids to a post-fusion solid-like state is an essential step in the post-printing processing (Mironov et al. 2008; Mironov et al. 2009). Thus, accelerated tissue maturation immediately after tissue construct bioprinting is the main technological imperative and potential impediment for further progress in the development of the emerging field of organ printing technology. Although it has already been demonstrated that natural-like levels of tissue maturation in tissue engineered blood vessels (Konig et al. 2009) and tissue engineered heart valves (Balguid et al. 2009) can be achieved in vitro, it usually takes several months of bioreactor-based in vitro cultivation and conditioning to achieve desirable levels of tissue maturation. Perfusion bioreactor-based screening of tissue maturation factors is extremely labor and reagent intensive and requires special equipment. These factors impose obvious limits on large-scale systematic screening of candidate tissue maturation factors and identification of their optimal concentration and combination. Progress in defining the optimal combination of factors and conditions (designing a "maturogenic cocktail") that accelerate tissue maturation will be enabled through the development of a battery of cost-effective, high throughput tissue maturation screening methods. Screening of "maturogenic" factors must be also based on reliable quantitative in vitro assays. It has recently been shown that tissue spheroids incubated in vitro for different periods of time have different tissue fusion kinetics (Rago et al. 2009). Longer incubation of tissue spheroids in hanging drop cultures is associated with an increased level of tissue cohesion and maturation mediated by cell adhesion molecules such as cadherins (Steinberg and Takeichi 1994) as well as increased accumulation of extracellular matrix molecules such as fibronectin (Robinson et al. 2003) and collagen (Xu et al. 2007). Thus, it is reasonable to hypothesize that tissue spheroid fusion kinetics is reflective of the level of tissue maturation. Here, we report experimental testing of two simple quantitative tissue spheroid fusion-based in vitro screening assays of tissue maturation: i) a tissue spheroid envelopment assay and ii) a tissue spheroid fusion kinetics assay.

In order to test the suitability of our in vitro systems as quantitative high throughput assays of tissue maturation, two approaches were employed. First, tissue spheroids fabricated from mouse bone marrow and cardiac valve interstitial cells were incubated with known (TGFβ1) and candidate (serotonin) maturogenic factors to test the efficacy of this assay to quantitatively demonstrate differences in the biomaterial properties of treated versus untreated spheroids. In a second approach, tissue spheroids fabricated from dermal fibroblasts isolated from wild-type and periostin-null mice were used to test the influence of extracellular matrix composition on tissue maturation.

Mice were bred and maintained in the Animal Research Center of the Medical University of South Carolina. The Institutional Animal Care and Use Committee approved all experiments. Periostin-null mice were generated as previously described (Norris et al. 2007; Oka et al. 2007). For isolation and culture of mouse bone marrow cells, mice were humanely sacrificed by Isoflurane inhalation followed by cervical dislocation. Bone marrow cells were flushed from the femurs and tibiae, pooled and washed twice with Ca^{2+}- and Mg^{2+}-free phosphate-buffered saline (PBS, Invitrogen) containing 0.1% bovine serum albumin (BSA, Sigma-Aldrich, St. Louis, MO). The suspension was triturated, filtered through a 40 µm cell strainer then cell plated directly into a T25 flask. After 5 days the primary culture was washed with PBS, then trypsinized and replated at 2×10^5 cells/cm^2 in DMEM (Invitrogen, Carlsbad, CA) fortified with 10% FBS, 10% mouse serum (both from Atlanta Biologicals, Norcross, GA), penicillin/streptomycin and glutamine (Invitrogen, Carlsbad, CA). The

medium was changed every third day and cells were passaged when they reached 80% confluence. Cells were used for aggregate formation after 10 passages. For isolation and culture of adult murine cardiac valve interstitial cells, hearts were removed from C57BL/6 mice and atrioventricular valves were aseptically dissected free of myocardium and collected in a conical 15ml tube containing DMEM supplemented with 10% FBS on ice. After centrifugation, new medium containing 2.5 mg/ml Collagenase Type 2 (Worthington Biochem, Lakewood, NJ) was added and the tube was incubated overnight at 37°C. After overnight digestion, the cell suspension was washed and triturated then plated at 2×10^5 cells/ cm^2. Cells were used for aggregate fabrication after the 4th passage. For isolation and culture of mouse dermal fibroblasts, pinnae from wild type and periostin-null mice were harvested and washed in sterile PBS. Pinnae were finely minced under sterile conditions and transferred to 50 ml centrifuge tubes containing 2.5mg/ml collagenase type 2 in serum-free culture medium (DMEM fortified with 1%penicillin/streptomycin, 1% glutamine, 1% fungizone). The centrifuge tube was incubated for 2 hours at 37°C, followed by vigorous trituration. The cell suspension was passed through a 40 μm cell strainer, resuspended in complete culture medium (as above) and plated on tissue culture plastic at a density of 2.0×10^5 cells/ cm^2. Non-adherent cells were removed after one hour by gently decanting medium and replacing with fresh culture medium.

For tissue spheroid biofabrication, cells were harvested using Trypsin/EDTA. Cells were enumerated and adjusted to a concentration of 1.6×10^6 cells/ml. In experiments using bone marrow- and cardiac valve-derived aggregates, cells were labeled with CellTracker[TM] Red CMTPX (for control cells) or CellTracker[TM] Green CMFDA (for maturogen-treated cells) (both reagents from Invitrogen, Carlsbad, CA) according the manufacturer's protocol before placing cells in hanging drops for aggregate formation. Droplets of cell suspension (25μl) were placed on the lid of a Petri dish that was inverted and incubated at 37°C. Medium was changed every 3 days. Micrographs were taken at 12 hour intervals using a Dage-MTI RC300 camera mounted on a Leica MZ12 stereomicroscope to monitor compaction of the spheroids. After seven days, two spheroids (control: control or control: TGFβ1/serotonin-treated) were placed in contact with one another in hanging drop culture and incubated for an additional 3 days. Imaging of spheroid envelopment was performed on a Leica DMI4000B inverted microscope equipped epifluorescence optics and a Hamamatsu Orca camera. Images were captured using a Leica HCX PL Fluotar 20× objective and processed with Adobe Photoshop. Next, the percentage of diameter of the treated aggregate that was covered (enveloped) by the control aggregate was measured using ImageJ (Abramoff et al. 2004). For each group (control, TGFβ1, serotonin), twenty fusing aggregates were measured. Immunofluorescence analysis of collagen production using a monoclonal antibody to the collagen chaperone Hsp47 (clone M16.10A1, Calbiochem, San Diego, CA) was performed on spheroids biofabricated from valve interstitial cells. Immunostaining with Hsp47 was performed after fixation with 4% PFA for 20 minutes, followed by permeabilization with 0.1% Triton X-100. Cy5-conjugated donkey anti-mouse IgG secondary antibody was used to immunolocalize biding of anti-Hsp47. In the fusion experiments using dermal fibroblast aggregates, two spheroids (both wild type or both periostin-null) were placed in contact with one another in hanging drop culture. The spheroids were photographed after 12, 24, 48 and 72 hours do document degree of spheroid fusion. Two sets of measurements were made; the longest diameter of the fusing aggregates and the length of contact area was measured for each set of aggregates at the indicated time points. Fifteen sets of aggregates from both wild-type and periostin-null fibroblasts were measured.

Tissue spheroids incubated in presence of TGFβ1 or serotonin (Figure 1) were more cohesive and as result were enveloped by tissue spheroids that were not incubated in the presence of maturogenic factors (Figure 1a-j). Measurement of envelopment indicated that

both TGFβ1- and serotonin-treated spheroids were enveloped an average of forty-percent by control (untreated) spheroids whereas as control spheroids were only enveloped an average of 10% by another control spheroid. Further, tissue spheroids treated with maturogenic factors exhibited greater collagen synthesis than did control spheroids (Figure 1k,l) as evidenced by detection of Hsp47, an intracellular chaperone of collagen types I-IV (Nagata 2003). These date indicate that both TGFβ1 and serotonin exhibit a fibrogenic or maturogenic effect in our tissue spheroid assay.

In our fusion kinetics assay, the kinetics of fusion of tissue spheroids fabricated from fibroblasts from wild-type mice was statistically different from spheroids fabricated from periostin-null mice (Figure 2). The length of the fusing aggregates as well as the length of the interface between them decreased much faster in tissue spheroids fabricated from periostin-null dermal fibroblasts compared to those from wild-type mice. Decreased tissue cohesion in periostin-null spheroids can be ascribed to the decrease in collagen fibrillogenesis that we have previously reported in periostin-null mice (Norris et al. 2007). Collectively, these findings indicate that periostin is a fibrogenic or maturogenic factor.

Our data demonstrate that design and implementation of high throughput assays that are sensitive enough for systematic screening of maturogenic factors is feasible. The first assay demonstrates that simple comparison of the kinetics of tissue fusion of two non-induced and two induced tissue spheroids can be compared to evaluate the maturogenic activity of a specific agent. In the experiments described above, we used tissue spheroids fabricated from fibroblasts isolated from wild-type and periostin-null mice to evaluate the maturogenic properties of the matricellular glycoprotein periostin. We have previously reported that periostin induces collagen fibrillogenesis (Norris et al. 2007). Also, it has recently been demonstrated that more mature tissue spheroids exhibit slower kinetics of tissue fusion (Norris et al. 2007). Thus, it is logical to assume that tissue spheroids fabricated with fibroblasts isolated from periostin-null mice will have a lower level of tissue cohesiveness and tissue maturity due to lower levels of collagen fibrillogenesis. Therefore, spheroids made from periostin-null fibroblasts should undergo fusion more rapidly than those made from wild-type fibroblasts. Indeed, this is the case. Our data demonstrate a statistically significant difference in the tissue fusion kinetics of tissue spheroids biofabricated from fibroblasts isolated from periostin-null and wild-type mice. These findings are in agreement with the previously reported fibrogenic role of periostin (Norris et al. 2007) and strongly suggest that ectopic expression of periostin can potentially be used as a maturogenic factor for accelerated tissue maturation in tissue engineering.

In the second envelopment assay, we showed that the measurable level of overlapping (envelopment) could be used as quantitative measure of tissue maturation. Although this tissue overlapping assay is not novel, it has to date been used predominantly as a qualitative assay (Steinberg and Takeichi 1994). During fusion of the two tissue spheroids, less cohesive tissue spheroids enveloped those with a higher level of tissue cohesiveness. Measurement of relative overlap is technically easy and it provides a reliable quantitative parameter for measurement. Our data demonstrate that the maturogenic factors (TGFβ1 and serotonin) induced accumulation of collagen in the tissue spheroids leading to changes in their cohesive properties and as a consequence, their enveloping behavior. This enveloping behavior of two tissue spheroids with different levels of tissue cohesiveness has been elegantly explained in biophysical and thermodynamic terms by Steinberg and Takeichi as the consequences of interfacial and surface tensional forces (Steinberg and Takeichi 1994; Jakab et al. 2008). Additional studies of the correlation of the enveloping behavior of tissue spheroids combined with measurement of their surface tension and viscosity will provide a broader understanding and elucidation of the biophysical basis for this reported behavior. However, our data demonstrate that this in vitro quantitative envelopment assay is suitable

for screening potential maturogenic factors. Interestingly, while the fibrogenic role of TGFβ1 is well known (Jian et al. 2002); that serotonin can act as a maturogenic factor is a novel finding. Serotonin is a natural vasoactive molecule and well-known mediator of neural activity. Our studies strongly suggest that serotonin has fibrogenic activity, which is in agreement with reports of the involvement of serotonin to the pathogenesis of fibrotic valvulopathies (Jian et al. 2002). Serotonin is relatively inexpensive compared to other growth factors, non-toxic and also induces proliferation of endothelial, smooth muscle and fibroblast cells (Jian et al. 2002). Thus, it could potentially be included as a component of a cocktail for accelerated tissue maturation of bioprinted organ constructs.

Use of these assays in combination with genomics and proteomics as well as systematic biochemical and immunohistochemical analyses will enable us to elucidate the molecular and cellular mechanisms of vascular tissue maturation and identify an optimal combination of factors that promote tissue maturation (a "maturogenic cocktail"). Additionally, use of reporter genes (for example, EGFP expression driven by the collagen type I promoter) will permit non-invasive biomonitoring of tissue maturation in real time and correlate the fusogenic, biochemical and material properties of self-assembling vascular tissue spheroids.

Conclusion

We have presented two simple quantitative in vitro assays suitable for large-scale high throughput screening of potential maturogenic factors. Compared to traditional perfusion bioreactor-based approaches, these assays are faster, more cost-effective and permit the systematic analysis of multiple "maturogenic" factors singly or in combination. Further, our data illustrate the potential feasibility of developing a technological platform for systematic high throughput maturogenic factor screening and design of an optimal cocktail of factors for acceleration of tissue maturation.

Acknowledgments

References

Abramoff MD, Magelhaes PJ, et al. Image processing using imageJ. Biophotonics International. 2004; 11(7):36–42.

Balguid A, Mol A, et al. Hypoxia induces near-native mechanical properties in engineered heart valve tissue. Circulation. 2009; 119(2):290–7. [PubMed: 19118259]

Jakab K, Damon B, et al. Relating cell and tissue mechanics: implications and applications. Dev Dyn. 2008; 237(9):2438–49. [PubMed: 18729216]

Jakab K, Neagu A, et al. Engineering biological structures of prescribed shape using self-assembling multicellular systems. Proc Natl Acad Sci U S A. 2004; 101(9):2864–9. [PubMed: 14981244]

Jakab K, Norotte C, et al. Tissue engineering by self-assembly of cells printed into topologically defined structures. Tissue Eng Part A. 2008; 14(3):413–21. [PubMed: 18333793]

Jian B, Xu J, et al. Serotonin mechanisms in heart valve disease I: serotonin-induced up-regulation of transforming growth factor-beta1 via G-protein signal transduction in aortic valve interstitial cells. Am J Pathol. 2002; 161(6):2111–21. [PubMed: 12466127]

Konig G, McAllister TN, et al. Mechanical properties of completely autologous human tissue engineered blood vessels compared to human saphenous vein and mammary artery. Biomaterials. 2009; 30(8):1542–50. [PubMed: 19111338]

Marga F, Neagu A, et al. Developmental biology and tissue engineering. Birth Defects Res C Embryo Today. 2007; 81(4):320–8. [PubMed: 18228266]

Mironov V, Boland T, et al. Organ printing: computer-aided jet-based 3D tissue engineering. Trends Biotechnol. 2003; 21(4):157–61. [PubMed: 12679063]

Mironov V, Kasyanov V, et al. Organ printing: promises and challenges. Regen Med. 2008; 3(1):93–103. [PubMed: 18154465]

Mironov V, Visconti RP, et al. Organ printing: tissue spheroids as building blocks. Biomaterials. 2009; 30(12):2164–74. [PubMed: 19176247]

Nagata K. HSP47 as a collagen-specific molecular chaperone: function and expression in normal mouse development. Semin Cell Dev Biol. 2003; 14(5):275–82. [PubMed: 14986857]

Norris RA, Damon B, et al. Periostin regulates collagen fibrillogenesis and the biomechanical properties of connective tissues. J Cell Biochem. 2007; 101(3):695–711. [PubMed: 17226767]

Oka T, Xu J, et al. Genetic manipulation of periostin expression reveals a role in cardiac hypertrophy and ventricular remodeling. Circ Res. 2007; 101(3):313–21. [PubMed: 17569887]

Rago AP, Dean DM, et al. Controlling cell position in complex heterotypic 3D microtissues by tissue fusion. Biotechnol Bioeng. 2009; 102(4):1231–41. [PubMed: 19012266]

Robinson EE, Zazzali KM, et al. Alpha5beta1 integrin mediates strong tissue cohesion. J Cell Sci. 2003; 116(Pt 2):377–86. [PubMed: 12482923]

Steinberg MS, Takeichi M. Experimental specification of cell sorting, tissue spreading, and specific spatial patterning by quantitative differences in cadherin expression. Proc Natl Acad Sci U S A. 1994; 91(1):206–9. [PubMed: 8278366]

Xu Q, Norman JT, et al. In vitro models of TGF-beta-induced fibrosis suitable for high-throughput screening of antifibrotic agents. Am J Physiol Renal Physiol. 2007; 293(2):F631–40. [PubMed: 17494090]
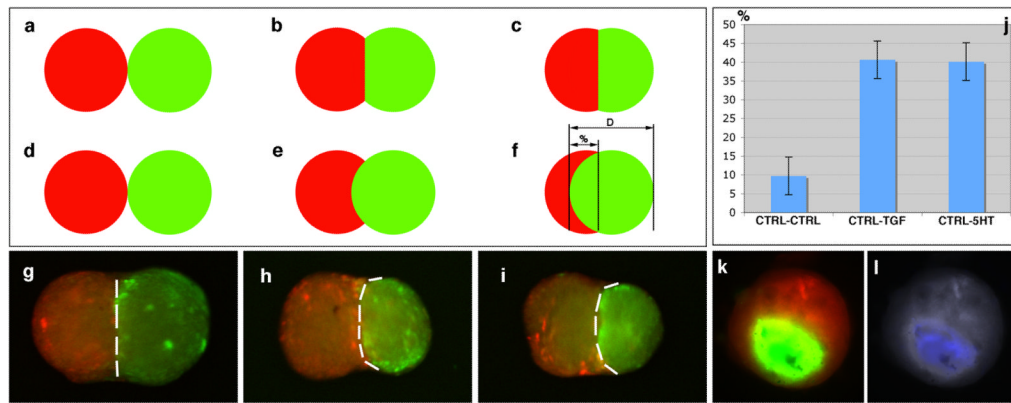
Figure 1.
Tissue spheroid envelopment assay using fluorescently labeled cells. **a-f.** Model quantitative assessment of spheroid envelopment. D = diameter, % = percent of envelopment. **g-i.** Tissue spheroids biofabricated from bone marrow cells after 72 hours exposure to control (g) medium, TGFβ1 (h), and serotonin (i). In panels h and i, control aggregates are red, while maturogen-treated aggregates are green. **j.** Percent envelopment of spheroids in response to maturogenic factors (TGFβ1, serotonin). **k.** Envelopment of spheroids biofabricated from cardiac valve interstitial cells. **l.** Immunodetection of HSP47 (a marker of collagen synthesis) in spheroids biofabricated from cardiac valve interstitial cells.
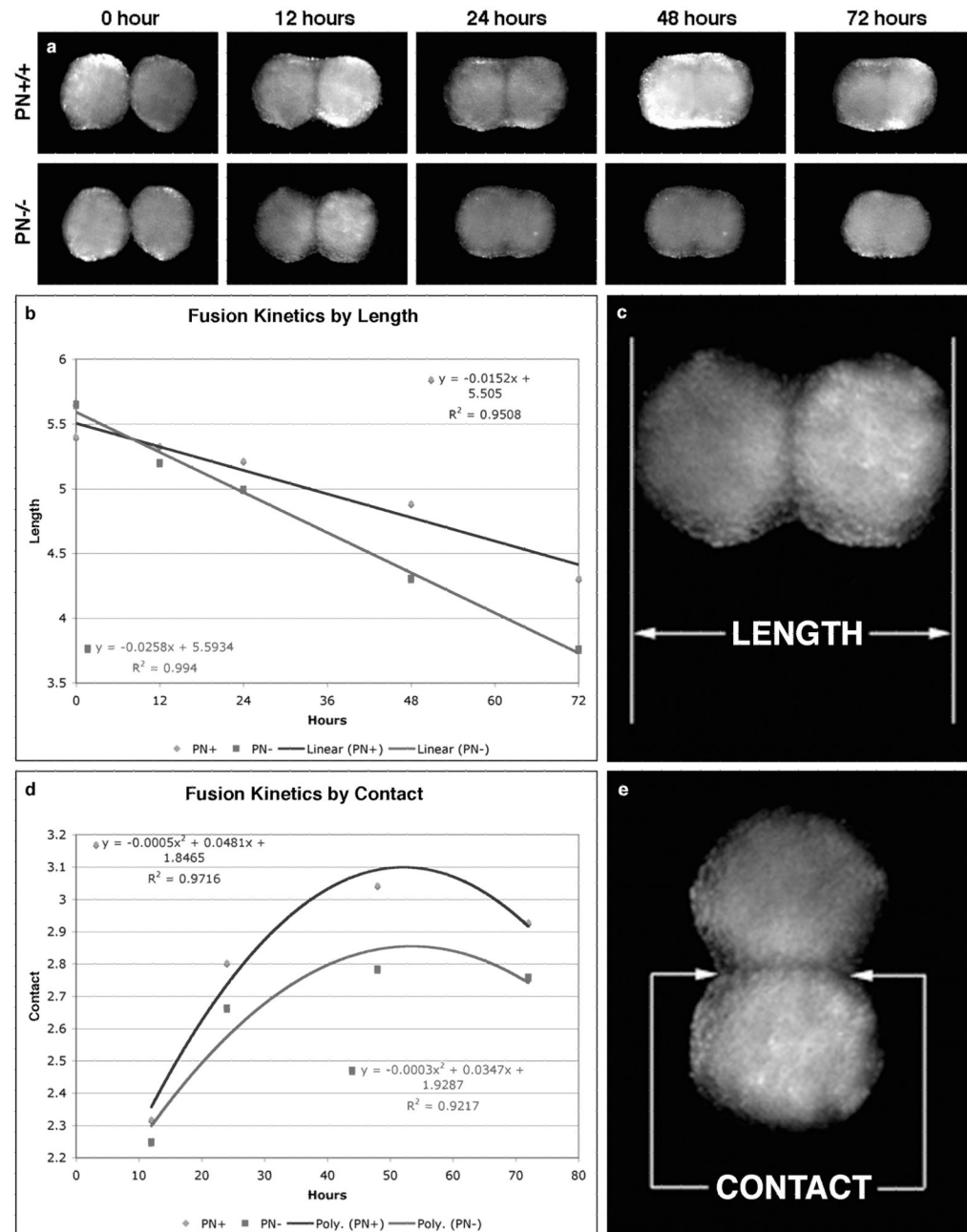
Figure 2.
Tissue spheroid fusion assay using wild-type and periostin-null dermal fibroblasts. **a.** Fusion of wild-type and PN-null spheroids biofabricated from dermal fibroblasts, imaged over 72-hours. **b,c.** Fusion kinetics by overall length (Blue = wild-type; red = PN-null). **d, e.** Fusion kinetics by contact region (Blue = wild-type; red = PN-null).